invited review

Structure and function of aquaporin water channels

A. S. VERKMAN¹ AND ALOK K. MITRA²

¹Departments of Medicine and Physiology, Cardiovascular Research Institute, University of California, San Francisco 94143-0521; and ²Department of Cell Biology, the Scripps Research Institute, La Jolla, California 92037

> Verkman, A. S., and Alok K. Mitra. Structure and function of aquaporin water channels. Am. J. Physiol. Renal Physiol. 278: F13-F28, 2000.—The aquaporins (AQPs) are a family of small membrane-spanning proteins (monomer size ~30 kDa) that are expressed at plasma membranes in many cells types involved in fluid transport. This review is focused on the molecular structure and function of mammalian aquaporins. Basic features of aquaporin structure have been defined using mutagenesis, epitope tagging, and spectroscopic and freeze-fracture electron microscopy methods. Aquaporins appear to assemble in membranes as homotetramers in which each monomer, consisting of six membrane-spanning α-helical domains with cytoplasmically oriented amino and carboxy termini, contains a distinct water pore. Mediumresolution structural analysis by electron cryocrystallography indicated that the six tilted helical segments form a barrel surrounding a central pore-like region that contains additional protein density. Several of the mammalian aquaporins (e.g., AQP1, AQP2, AQP4, and AQP5) appear to be highly selective for the passage of water, whereas others (recently termed aquaglyceroporins) also transport glycerol (e.g., AQP3 and AQP8) and even larger solutes (AQP9). Evidence for possible movement of ions and carbon dioxide through the aquaporins is reviewed here, as well as evidence for direct regulation of aquaporin function by posttranslational modification such as phosphorylation. Important unresolved issues include definition of the molecular pathway through which water and solutes move, the nature of monomer-monomer interactions, and the physiological significance of aquaporin-mediated solute movement. Recent results from knockout mice implicating multiple physiological roles of aquaporins suggest that the aquaporins may be suitable targets for drug discovery by structure-based and/or high-throughput screening strategies.

> $water\ transport;\ protein\ structure;\ electron\ microscopy;\ crystallography;\ water\ permeability$

THE AQUAPORIN FAMILY of water channels consists of 10 proteins cloned from mammals and many more from amphibians, plants, yeast, bacteria, and various lower organisms. There has been considerable interest in the biology of aquaporins (AQPs) with more than 500 studies published over the past 5 years on aquaporin cloning, genetics, tissue localization, developmental and regulated expression, transgenic mouse models, and structure/function analyses. This review is focused on recent data concerning the structure and function of mammalian aquaporins. Although a substantial body of research about aquaporin structure and function has been completed, there remain many fundamental unre-

solved issues, some of which will be very challenging to address. This review critically evaluates existing and new information, pointing out unresolved and controversial issues as well as directions for future work.

The aquaporins are small, very hydrophobic, intrinsic membrane proteins. Kyte-Doolittle hydropathy plots of the aquaporin amino acid sequences are similar, showing at least six nonpolar regions of sufficient length to span the membrane (Fig. 1, A and B). Predicted monomer sizes of the mammalian aquaporins range from 26 to 34 kDa. Sequence alignment of the aquaporins show several highly conserved motifs, including two "NPA" sequences, and single "AEFL" and "HW[V/I][F/Y]WXGP"

F14 INVITED REVIEW

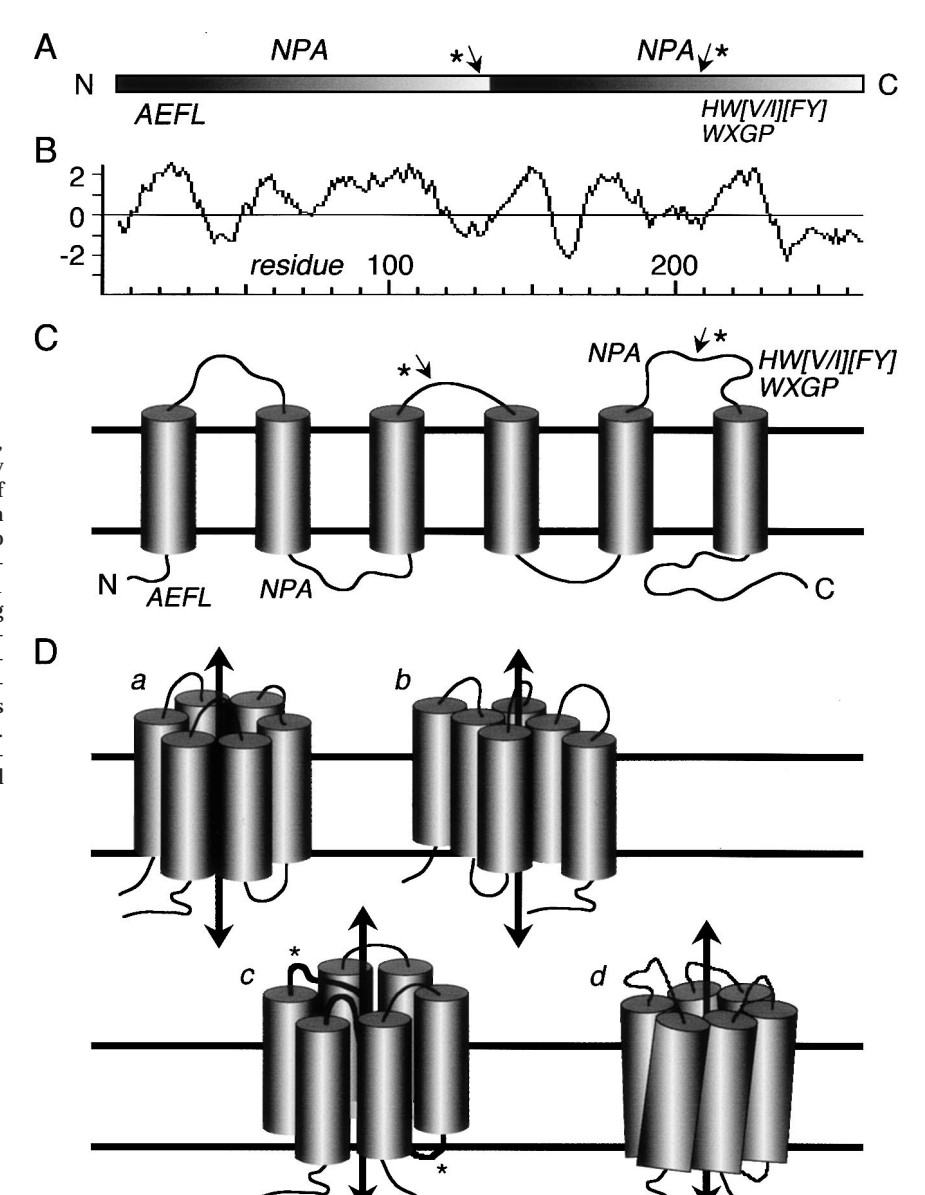


Fig. 1. Cartoon of aquaporin (AQP) primary, secondary, and tertiary structure. A: primary structure of an aquaporin, showing locations of conserved amino acid sequences, the tandem repeat motif, and locations of additional amino acids (denoted by asterisks) in the aquaglyceroporins. B: Kyte-Doolittle hydropathy plot of AQP1 with positive values on the ordinate indicating hydrophobic regions. C: topology cartoon showing 6 membrane-spanning helical domains, cytoplasmic-facing amino and carboxy termini, locations of conserved NPA sequences, and locations of additional amino acids in aquaglyceroporins. D: possible tertiary disposition of helical segments. Water pathway shown as a double-headed arrow. See text for explanations.

sequences. Overall amino acid identities among the mammalian aquaporins range from 19 to 52%. Within the mammalian aquaporin family, two subgroups have been defined: "aquaporins" and "aquaglyceroporins," "HW[V/I][F/Y]WXGP" sequences. Overall amino acid with the latter transporting glycerol and sometimes larger molecules in addition to water (see below). Compared with the sequence of the aquaporins (AQP1, AQP2, AQP4, AQP5, AQP6, and AQP8), the aquaglyceroporins (AQP3, AQP7, and AQP9) contain two additional peptide spans as indicated in Fig. 1A. Further analysis of aquaporin sequences indicates homology between the first and second halves of the molecule (114), suggesting evolution of aquaporin genes from an intragenic duplication event. This tandem repeat motif has implications concerning aquaporin structure as described below.

The hydropathy profiles of the aquaporins suggest six putative helical domains (Fig. $1\,C$). Work from

several laboratories utilizing epitope tagging, aquaporin-reporter chimeras, and site-specific antibodies confirmed this basic topological organization and indicated that the NH₂ and COOH termini are cytoplasmically oriented (4, 81, 88, 91). Several of the aquaporins have consensus sequences for *N*-linked glycosylation and are monoglycosylated in native tissues. Biochemical analysis of purified human erythrocyte AQP1 indicated that 50% of AQP1 monomers are glycosylated with a polylactosaminyl oligosaccharide of 5.4 kDa at residue N42 in the first extracellular loop (102). However, glycosylation does not appear to be important for aquaporin function or membrane targeting (5, 102, 127). Although the six membrane-spanning motif shown in Fig. 1C probably applies to all aquaporins, it has been demonstrated experimentally only for AQP1, AQP2, and AQP4 (4, 81, 88). Various assemblies of the membranespanning domains have been proposed (50, 91). Cartoons a and b in Fig. 1D show an aqueous pore

comprising six and four transmembrane (TM) helices, respectively. *Cartoon c* in Fig. 1D shows an aqueous pore made up of six helices, but also containing additional extramembrane residues (denoted by an asterisk) within the pore. *Cartoon d* of Fig. 1D (see also Fig. 4) shows a barrel formed by tilted helical domains as deduced from electron crystallographic analyses described below.

Although not directly relevant to the topic of aquaporin structure and function, it is noted briefly that proteins other than aquaporins appear to be able to transport water. Osmotically induced water transport pathways have been demonstrated to be associated with the glucose transporter (32, 124), cAMP-activated cystic fibrosis transmembrane conductance regulator (CFTR) (41, 86), urea transporter UT3 (119), and multiple Na-solute cotransporters (65). These transporters thus appear to contain a continuously open aqueous lumen that in some cases may be gated. Because of the low membrane densities of these transporters compared with the aquaporins, it is unclear whether they can make a quantitatively significant contribution to total plasma membrane water permeability. In the case of Na-dependent cotransporters, Wright and colleagues (65, and references cited therein) have offered evidence to support the interesting hypothesis that energetically uphill water transport can occur by a cotransport mechanism in which one turnover of a cotransporter moves single Na and solute molecules accompanied by hundreds of water molecules. The generality and biological significance of their observations remain to be elucidated.

WATER TRANSPORT FUNCTION OF AQUAPORINS

Aquaporin-mediated water transport is generally measured using an osmotic swelling assay in *Xenopus* oocytes expressing an aquaporin cRNA. As originally described (125), quantitative image analysis is used to deduce the time course of oocyte swelling in response to a sudden decrease in extracellular solution osmolality from 200 to 0–100 mosmol/kgH₂O. Water transport in aquaporin-transfected mammalian cells has also been studied by a variety of biophysical approaches including stopped-flow light scattering (68), total internal reflection fluorescence microscopy (26), laser interferometry (29), and Fourier optics dark-field/phase-contrast microscopy (25). Stopped-flow light scattering has also been used to assay aquaporin-mediated water transport in vesicles derived from yeast (61) and in reconstituted proteoliposomes containing purified aquaporin proteins (100, 122).

The intrinsic "single-channel" aquaporin water permeability can be computed from proteoliposome size, the kinetics of volume change following an osmotic challenge, and the amount of aquaporin protein in the proteoliposome. The single-channel water permeability of AQP1 was determined to be $\sim 6 \times 10^{-14}$ cm³/s (100). This value has several implications. If the aquaporin water channel is a narrow cylindrical pore that permits single-file water transport, then classic theory (31) predicts a channel diameter of 3.8 Å (126). Although

such theoretical treatments clearly represent a gross oversimplification, it is notable that a 3.8-A-diameter pore can pass water but not larger molecules, as found experimentally. Moreover, since the observable osmotic water permeability coefficient (P_f) of a membrane is the product of the single-channel water permeability and the aquaporin membrane density, a substantial increment in $P_{\rm f}$ (0.01 cm/s) over baseline (lipid-mediated) $P_{\rm f}$ (0.001–0.004 cm/s) would require an AQP1 membrane protein density of at least 1,000 aquaporin monomers per square micrometer. This is remarkably greater than the typical membrane density of ion channels, with generally <1 channel/ μm^2 except in specialized cases such as the acetylcholine receptor in postsynaptic membranes. Therefore, the low intrinsic water permeability of aquaporins, which is limited by biophysical constraints on fluid movement, requires the expression of many aquaporins for functional significance. A consequence of the high-density aquaporin expression is that leaks to solutes and ions, even if small, could have deleterious effects on the cell interior. For example, if kidney AQP2 were permeable to protons, then the acidic urine bathing the collecting duct lumen would produce profound intracellular acidification.

The expression of aquaporins in oocytes permitted quantitative analysis of single-channel water permeabilities (118). AQP0-AQP5 were tagged with c-myc or FLAG epitopes at their NH₂ or COOH termini and expressed in oocytes. (AQP0 is MIP, the major intrinsic protein of lens fiber.) Oocytes were assayed for osmotic water permeability by the swelling assay and in parallel for plasma membrane aquaporin expression by quantitative immunofluorescence microscopy. It was found that AQP4 had substantially higher intrinsic water permeability than AQP1, AQP2, and AQP5 and that AQP3 and AQP0 had the lowest intrinsic water permeabilities. The high intrinsic water permeability of AQP4 was confirmed in reconstituted proteoliposomes containing AQP4 purified from heterologously expressing insect cells (117). The low intrinsic water permeability of AQPO has also been reported by Chandy et al. (14). Recently, Meinild et al. (73) measured the very early swelling and shrinking of oocytes expressing aquaporins in response to osmotic and solute gradients. They confirmed that water flow through AQP0-AQP5 is bi-directional and symmetric, as was known for many years for AQP1-mediated water transport in erythrocytes, and measured reflection coefficients for urea and glycerol. An interesting result was that solute reflection coefficients for most aquaporins were near unity, whereas the glycerol reflection coefficient for AQP3 was very low (= 0.2). Assuming that unstirred layer and rapid solute permeation effects do not introduce uncertainty in the data interpretation, then the low glycerol reflection coefficient indicates a common water/glycerol pore through AQP3. It will be important to confirm this observation by solvent drag measurements (as done for UT3 in Ref. 119), in which osmotically induced water flow is predicted to drive the transport of radiolabeled glycerol.

F16 INVITED REVIEW

WATER/SOLUTE SELECTIVITY OF THE AQUAPORINS

Early studies of AQP1 reconstitution in proteoliposomes indicated that under conditions in which liposome water permeability was increased >100-fold compared with control liposomes, there was no increase in urea or proton permeabilities (100, 122). No ion conductances were detected in two-electrode voltage-clamp measurements of AQP1-AQP4 (35, 40, 45, 67, 80, 126). Thus some aquaporins appear to be able to pass water efficiently while excluding small solutes. Although steric hindrance has been proposed to explain the water selectivity of aquaporins, it is very likely that additional factors such as electrostatic interactions and hydrogen bonding are responsible for the absence of proton and ion conductances.

Radioactive solute uptake studies in oocytes indicated that AQP3 and AQP7 transport glycerol and to some extent urea, along with water (24, 44, 45, 67). Echevarria et al. (23) investigated whether water and glycerol move through a common pathway in oocytes expressing AQP3. On the basis of different temperature dependences of water and glycerol transport, as well as different inhibitor profile, it was concluded that water and glycerol do not share the same pathway through AQP3. This result appears to be contradicted by the finding of a low reflection coefficient for glycerol transport by AQP3 in oocytes (73), implying a common water/glycerol pathway. Kuwahara et al. (56) also concluded that water and glycerol share a common pathway through AQP3 based on similar effects of mutagenesis on water and urea transport.

Tsukaguchi et al. (96) reported that AQP9, which is expressed most strongly in hepatocytes, is able to transport water along with a wide variety of solutes including carbamides, polyols, purines, and pyramidines. The measurement of low-reflection coefficients suggested a common water/solute pathway. They proposed that AQP9 may provide an aqueous pore through which many types of molecules cross cell membranes with minimal osmotic perturbation. These exciting findings mandate further confirmation and extension.

It was recently suggested that AQP1 can also transport carbon dioxide. Nakhoul et al. (77) reported that oocytes expressing AQP1 had ~40% increased CO₂ permeability compared with control oocytes. Using pH-sensitive microelectrodes, they found an increased rate of acidification in AQP1-expressing oocytes in response to external addition of CO₂/HCO₃. It was necessary to microinject oocytes with carbonic anhydrase to convert the increase in oocyte CO2 content to a measurable change in pH. They concluded that either AQP1 directly transported CO₂ or that AQP1 expression indirectly altered membrane CO₂ permeability in oocyte membranes. Follow-up work from the same group (17) showed HgCl₂ inhibition of CO₂ transport by AQP1 in oocytes but not by an AQP1 mutant (C189S) that lacks the cysteine known to be involved in water transport inhibition. Another recent report demonstrated CO₂ transport through AQP1 in reconstituted proteoliposomes (79). A consequence of these finding is

that AQP1-mediated CO₂ transport might be important in lung gas exchange because AQP1 is strongly expressed in pulmonary capillary endothelia and erythrocytes. To investigate this possibility in an animal model, we recently measured CO₂ transport in lungs in anesthetized ventilated wild-type and AQP1-deficient mice (116). The time course of arterial blood-gas CO₂ was measured in response to an acute change in inspired gas CO₂ content. There was no difference in lung CO₂ transport in wild-type vs. AQP1 null mice. In addition, we were unable to demonstrate significant differences in CO₂ transport in erythrocytes from wildtype vs. AQP1 null mice, and we did not find a detectable increment in CO2 permeability in AQP1reconstituted vs. control liposomes despite a >150-fold increase in water permeability. Further work is needed to determine the role of other aquaporins in gas transport.

REGULATION OF AQUAPORIN FUNCTION

The regulation of water permeability in kidney collecting duct cells expressing AQP2 is well characterized. Water permeability is primarily regulated by a cAMPdependent vesicular trafficking mechanism in which functional AQP2 water channels are inserted into the cell plasma membrane (reviewed in Ref. 72). There is indirect evidence that AQP1 trafficking in intrahepatic cholangiocytes may also be regulated by cAMP (71). However, with the exception of AQP2 and AQP6 (120), the other aquaporins appear to be constitutively expressed at the plasma membrane. In addition to regulated vesicular trafficking, other water transport regulatory mechanisms include transcriptional regulation and posttranslational modification. Transcriptional regulation clearly occurs for AQP2 (72) and possibly for other aquaporins.

Several of the aquaporins contain consensus sequences for phosphorylation by protein kinases A and C. The function of several plant aquaporins is believed to be regulated by phosphorylation. Recently, it was shown that water permeability of PM28A from spinach leaf plasma membranes was regulated by phosphorylation of two serine residues, and that the in vivo phosphorylation state was sensitive to the external water potential (49). There have been reports that raised the issue of direct regulation of mammalian aquaporin function by phosphorylation. Youl et al. (121) reported that cAMP activated AQP1 water transport in oocytes and induced a cation conductance. However, subsequent studies by several laboratories using different approaches did not confirm this observation (1, 20, 108, 119). Kuwahara et al. (55) found a small increase in AQP2-mediated water transport in an oocyte expression system and suggested direct regulation of AQP2 function by phosphorylation. However, this finding was not confirmed in measurements on AQP2-containing oocytes (118) or kidney endosomes (63). Patil et al. (78) reported that water permeability in oocytes expressing AQP1 was increased by vasopressin and decreased by

atrial natriuretic peptide; however, the significance of these data must await the identification of appropriate receptors in oocytes. This group also reported decreased water permeability in AQP4-expressing oocytes treated with a phorbol ester, implicating an effect of phosphorylation on function (38). We have not been able to confirm this finding in oocytes (118) or stably transfected CHO cells (unpublished results). Recently, pH-dependent regulation of aquaporin function has been suggested for AQP0 (12) and AQP6 (120). In the case of AQP6, an anion conductance appearing at low pH was found. However, transport properties measured in oocytes and under nonphysiological conditions should be viewed cautiously.

ULTRASTRUCTURAL ANALYSIS OF AQUAPORINS

Freeze-fracture electron microscopy (FFEM) provided the first low-resolution view of aquaporins. AQP1 ultrastructure was studied in reconstituted proteoliposomes containing purified AQP1, AQP1-transfected CHO cells, and native kidney proximal tubule and thin descending limb of Henle. Rotary shadowing FFEM revealed that membranes in each of these preparations contained disorganized intramembrane particles (IMPs) of \sim 8.5 nm diameter (104); each IMP appeared to consist of a tetrameric assembly of individual units (thin descending limb of Henle and AQP1 proteoliposomes shown in Fig. 2, A and B). Making assumptions

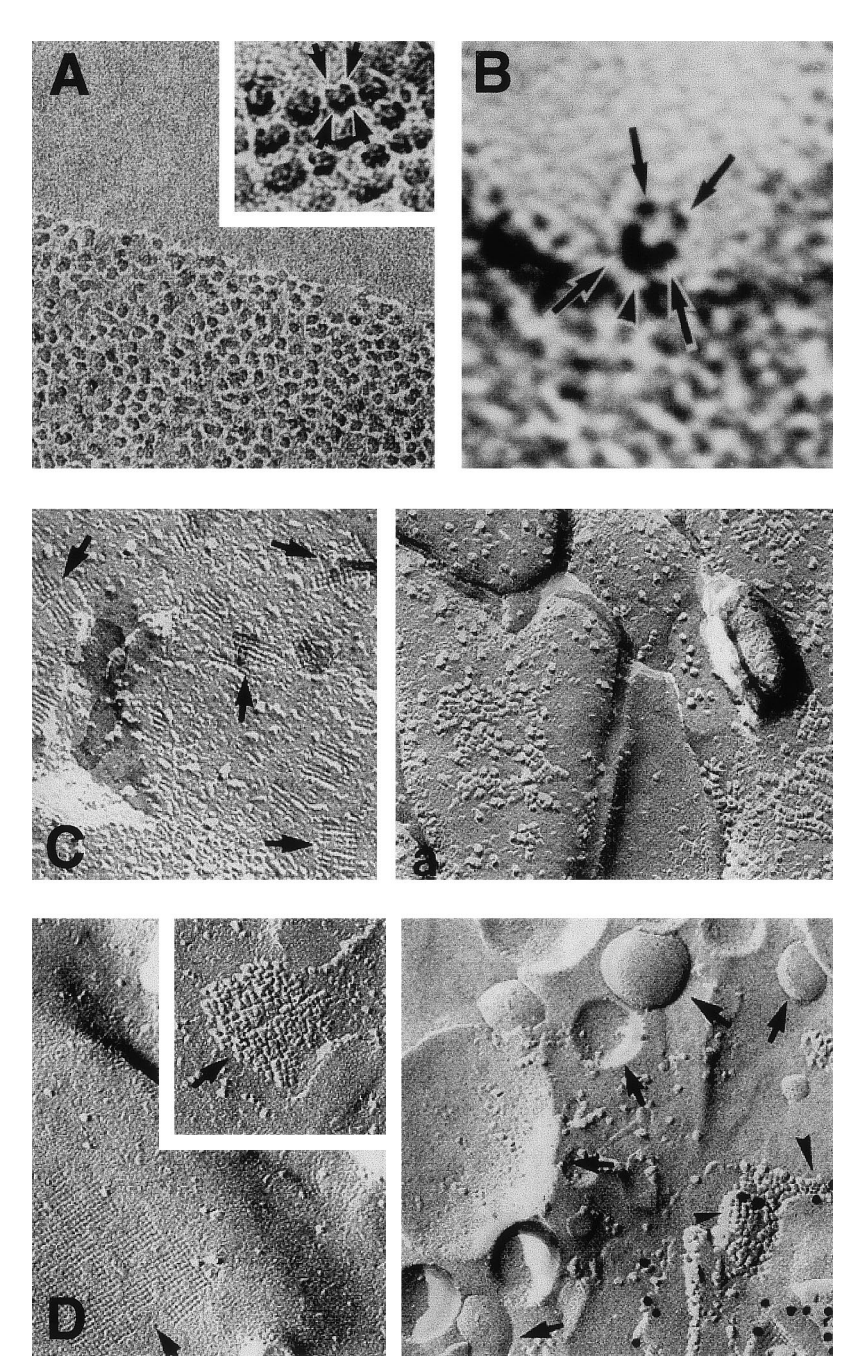


Fig. 2. Aquaporin ultrastructure studied by freeze-fracture electron microscopy. *A*: high density of intramembrane particles at the apical membrane of thin descending limb of Henle; *inset* shows tetrameric appearance. *B*: high-magnification view of AQP1 tetramer in a reconstituted proteoliposome containing purified human erythrocyte AQP1 protein. *C*: freeze fracture of basolateral membrane of kidney collecting duct showing orthogonal arrays of particles (OAPs) on E-face (*left*) and P-face (*right*). *D*: OAPs in AQP4-expressing CHO cells (*left*); label fracture (*right*) showing immunogold labeling of OAPs by anti-AQP4 antibody. Adapted from Refs. 104 and 105.

F18 INVITED REVIEW

about AQP1 monomer density and length, we computed that an AQP1 tetramer would have an apparent largest diameter of 7.2 nm, which agreed with the FFEM data after correction for the thin (\sim 1 nm) platinum coat added during the shadowing procedure. These results suggested that AQP1 is assembled as homotetramers in membranes. Definitive identification of the IMPs in kidney cell membranes came from FFEM studies of kidney in AQP1 knockout mice (21). In plasma membranes from thin descending limb of Henle, the IMP density was 6.5-fold lower in knockout vs. wild-type mice, and the IMPs in wild-type but not knockout mice had the characteristic AQP1 IMP diameter and tetrameric appearance.

A distinct morphological pattern of IMPs, called orthogonal arrays of particles (OAPs), has been observed by FFEM in many tissues, including the basolateral membrane of kidney collecting duct epithelia, astroglial cells in the central nervous system, skeletal muscle plasmalemma, and other tissues. OAPs are seen as regular square arrays with a characteristic cobblestone pattern on E-face and P-face FFEM (Fig. 2C). The density of OAPs was found to be altered in various forms of dementia and Duchenne's muscular dystrophy; however, the identity and function of the OAPs were not known. On the basis of the finding that AQP4 was present in the same cell types in which OAPs were identified, we proposed in 1995 that AQP4 is the OAP protein (34). Support for this hypothesis came from FFEM on stably transfected CHO cells expressing functional AQP4 (115). OAPs with large patch sizes were found with essentially identical ultrastructure to those seen in mammalian cells. Figure 2D shows immunogold label fracture of OAPs in AQP4-transfected CHO cells. Direct evidence that AQP4 is the OAP protein in vivo came from freeze-fracture studies on kidney, skeletal muscle, and brain from AQP4 knockout mice (105). OAPs were identified in every sample from wild-type and AQP4 heterozygous mice and in no sample from AQP4 knockout mice. Subsequent label fracture of OAPs in brain tissue confirmed that OAPs are composed of AQP4 (84). These results established the identity and function of OAPs as AQP4 water

It is not clear why AQP4 and MIP form OAPs, whereas other aquaporins studied (AQP1, AQP2, AQP3, and AQP5; Ref. 103) do not. Sequence alignments of OAP-forming vs. non-OAP-forming aquaporins have not been informative in identifying contact surfaces that could energetically stabilize OAP assembly (unpublished work). It was proposed that the organization of AQP4 in OAPs might augment water transport function through a bulk-flow siphoning mechanism (115). As mentioned above, AQP4 has greater intrinsic water permeability than the other aquaporins, despite its selectivity for water transport. It was recently postulated that the colocalization of OAPs comprising AQP4 and K+ channels in retinal Muller cells might facilitate local water fluxes associated with K⁺ siphoning (76). Thus far, these possibilities remain unsubstantiated. It will be useful to measure the intrinsic water permeability of AQP4 in OAPs vs. in disorganized IMPs as found for AQP1.

SPECTROSCOPIC ANALYSIS OF AQUAPORINS

Spectroscopic studies provided early information about aquaporin protein structure prior to investigations by electron crystallography. The first determination of the secondary structure content of purified AQP1 in membranes and detergents was done using circular dichroism and Fourier transform infrared spectroscopy (101). AQP1 was found to have 38-40% α -helical content and 40-43% β-sheet/turn. It was concluded that AQP1 monomers probably contain multiple membrane-spanning helical domains as found in bacteriorhodopsin. A β-barrel structure (as found in bacterial porins), which should have close to zero α -helical content, was thus ruled out. Subsequent Fourier transform studies by Haris et al. (39) and Cabiaux et al. (11) showed 36 and 42-48% α -helical content, respectively. It is noted that analyses of membrane protein secondary structure using circular dichroism and Fourier transform infrared spectroscopy are model dependent, because they require specification of a basis set of spectra for spectral deconvolution. There is considerable uncertainty in appropriate basis spectra because of the limited number of membrane proteins whose structures have been solved at atomic resolution.

Other spectroscopic techniques that have been applied to analyze protein structure/dynamics include resonance energy transfer, tryptophan fluorescence spectroscopy, and time-resolved fluorescence anisotropy. Resonance energy transfer can provide information about site-site distances with resolution better than 0.5 nm, provided that suitable donor and acceptor fluorescent labels can be incorporated into a purified functional protein. However, energy transfer has not been applied to study aquaporin structure. Measurement of tryptophan emission spectra and quenching properties provides information about the nature of the tryptophan environment such as its accessibility to water. Tryptophan spectroscopy of AQP1 revealed a nonpolar location for all four tryptophans (27). Quenching studies of membrane-incorporated *n*-anthroyloxy fatty acid probes provided a low-resolution map of the locations of the tryptophans within the bilayer. Measurement of time-resolved anisotropy provides information about the segmental mobility of a protein, as was applied to study pH-dependent conformations of the cytoplasmic tail in erythrocyte band 3 in situ (95). A preliminary study of AQP1 labeled with fluorescein at a cysteine residue defined picosecond and nanosecond segmental motions of AQP1 and suggested that mercurial binding is associated with a conformational change (28). Last, a single-photon radioluminescence (SPR) technique was applied to characterize the AQP1 aqueous pore. SPR is a novel biophysical method in which an electron from tritium radiodecay deposits energy in the vicinity of a fluorescent molecule (8, 87). Detection of a differential SPR signal from tryptophans in AQP1 arising from ³H₂O vs. [³H]methylglucose decay indicated the existence of an aqueous pore that ex-

cludes methylglucose (7). In summary, although spectroscopic approaches can provide biophysically elegant tools to define certain aspects of protein structure, they have not been particularly informative in elucidating high-resolution details of aquaporin structure. However, after high-resolution structural data are available, time-resolved anisotropy and resonance energy transfer methods may provide unique information about aquaporin intramolecular dynamics to complement static structural data.

MUTATIONAL ANALYSIS OF AQUAPORINS

Site-directed mutagenesis, domain swapping, and chimera expression studies have been done on several of the aquaporins. The general approach has been to express the mutated protein in *Xenopus* oocytes and measure water permeability using the swelling assay. A general limitation of this approach in aquaporin research is that the major function of aquaporins is water transport, which is characterized by a single value: the water permeability coefficient. In contrast, analysis of ion channel mutants provides many parameters such as open probability, gating kinetics, ion specificity, and current-voltage relationship. In addition, often the aquaporin mutants studied thus far do not fold correctly and consequently are impaired in their routing to the plasma membrane. A general caveat of mutagenesis studies is that mutation in one region of a molecule can affect function by an indirect global conformation change, so that it may not be correct to infer sitespecific effects. Nevertheless, several informative aquaporin mutagenesis studies have been reported. Point mutagenesis studies have identified critical cysteine residues responsible for the mercurial sensitivities of AQP1, AQP2, and AQP3 (4, 56, 82, 127). For AQP4, which is mercurial insensitive, cysteine-scanning mutagenesis has shown that particular residues near the conserved NPA motifs confer strong mercurial sensitivity to AQP4 and thus may line the aqueous pore (90). Several mutagenesis studies indicate that mutations near the NPA motifs alter aquaporin function (4, 50, 56, 81, 90), suggesting that this conserved region may be located at or near the water pathway.

Shi et al. (89) addressed the issue of whether individual AQP1 monomers in a tetramer contain separate water pores. Heterodimers containing wild-type and mutant AQP1 monomers were expressed in oocytes, and intrinsic water permeability was measured quantitatively as done in the study by Yang and Verkman (118). The water permeability properties of the heterodimers (intrinsic water permeability and mercurial sensitivity) reflected the additive/averaged properties of the individual monomers. Thus individual AQP1 monomers in a tetramer appear to function independently, suggesting that each monomer encloses a watertransporting pathway. The question remains as to why aquaporins assemble in tetramers. Whether significant monomer-monomer interactions, apparent in the threedimensional (3-D) structure of an aquaporin tetramer, play a role in generating functionally active pores in a monomer is not known. Also, it is not known whether

different aquaporins can spontaneously form heterotetramers in native membranes, such as AQP3 and AQP4 at the basolateral membrane of kidney collecting duct, as has been reported with different connexon isotypes forming heteroligomeric gap-junction channels in lens (48).

Recently, an interesting report (57) described that the replacement of a tyrosine and tryptophan by a proline and leucine in the sixth TM helix of an insect aquaporin (AQPcic) resulted in conversion from a waterselective transporter to a glycerol channel. The mutated residues were selected from sequence comparisons of aquaporins vs. aquaglyceroporins. In a separate study, the same group reported that the bacterial glycerol facilitator protein GlpF is monomeric in detergent micelles (58); introduction of specific mutations in AQPcic resulted in conversion from a tetramer to a monomer when solubilized in detergents. These results appear to have a number of interesting implications: that glycerol movement through an aquaporin occurs through the monomer rather than between monomers in a tetrameric assembly, that residues in the sixth TM helix are responsible for tetramer stabilization, and that water and glycerol share a common pathway. Similar mutagenesis studies are warranted in other aquaporins to evaluate the generality of these predic-

AQUAPORIN EXPRESSION AND PURIFICATION

Structural analysis by crystallographic methods requires purification of functional protein to near homogeneity. Purification of human AQP1 from native erythrocyte membranes is readily accomplished by membrane isolation following hypotonic shock, N-lauroylsarcosine stripping of non-AQP1 membrane proteins, detergent (Triton or octylglucoside) solubilization, and purification using anion exchange and/or phenylboronic acidagarose column chromatography (102). For AQP1 mutants and other aquaporins, a heterologous expression system is needed.

Progress has been made in the heterologous expression of aquaporins; however, it is too early to determine whether the expressed proteins will be suitable for crystallography. Using a Saccharomyces cerevisiae yeast expression system, Laize et al. (61) were the first to demonstrate moderate to high levels of expression of a recombinant aquaporin. The AQP1 cDNA was expressed using the inducible GAL10-CYC1 promoter in the NY17 yeast strain in which secretory vesicles accumulate in response to heat shock. The isolated secretory vesicles expressed functional AQP1. More recently, the same group expressed an NH2-terminal hemaglutinin-epitope (YPYDVPDY) (recognized by a monoclonal antibody) tagged AQP1 using the same expression system but omitting the heat shock (60). Tagged AQP1 at (~0.2 mg/l of yeast) was purified and shown to be functional. Working with secretory vesicles of S. cerevisiae strain SY1, Coury et al. (18) reported increased expression levels of both AQP1 and AQP2 by optimization of induction protocols to maximize protein expression. Subsequently, Lagree et al. (59) expressed F20 INVITED REVIEW

the recombinant insect aquaporin AQPcic using the W303.1B strain of *S. cerevisiae* under transcriptional control of GAL10-CYC1 promoter and used a procedure analogous to erythrocyte AQP1 purification to obtain purified, functional AQPcic. Recently, homologous expression of bacterial aquaporin AQPz from Escherichia coli has been reported (9). Using a baculovirus-Sf9 insect cell expression system, the mercurial-insensitive water channel AQP4 was overexpressed and purified to homogeneity (117). Proteoliposomes reconstituted with purified AQP4 protein were substantially more water permeable than proteoliposomes containing similar quantities of AQP1, yet water permeability in the AQP4 proteoliposomes was not inhibited by mercurials. To date, no structural data have been reported utilizing crystals obtained from a heterologously expressed aquaporin. For successful crystallization, it will be important to verify that all heterologously expressed and purified protein is properly folded and functional.

ELECTRON CRYSTALLOGRAPHY OF AQP1

Overview. To understand at the atomic level how a biological macromolecule functions, knowledge of its 3-D structure is essential. This has proven to be true for soluble proteins such as enzymes, electron transport proteins, and protein-nucleic acid assemblies such as viruses. Unlike soluble proteins, integral membrane proteins are usually recalcitrant to the growth of large, well-ordered 3-D crystals, which is necessary for highresolution X-ray crystallographic analysis. Recent examples of high-resolution (<4 Å) membrane protein structures determined by X-ray crystallography include the *E. coli* outer membrane transporter FepA (10), mechanosensitive ion channel from Mycobacte*rium tuberculosis* (13), *E. coli* ferrichrome-iron receptor FhuA (30), and Saccharomyces lividans K⁺ channel (22). Well-ordered 3-D crystals of AQP1 have been generated in the laboratory of our collaborator Dr. Michael Wiener (113). These crystals diffract X-rays to ~4 Å and are suitable for traditional X-ray crystallography.

An alternative approach is to generate thin, onemolecule thick 2-D crystals in lipid bilayers (reviewed in Refs. 42, 47, 53) and apply electron crystallography to solve the protein structure. Examples of membrane protein structures solved to atomic resolution by electron crystallography of 2-D crystals in the lipid bilayer include the LHC II from spinach chloroplasts (54) and bacteriorhodopsin from Halobacterium salinarium (50, 52, 74). The membrane protein in such a 2-D crystal is surrounded by lipids rather than detergent micelles, which allows for a direct assay of function such as solute transport (110) and its modulation such as ligand-gated channel opening (6, 98). Another notable advantage of electron crystallography is that phases can be obtained directly from images, whereas X-ray crystallography requires additional experimental methods such as isomorphous replacement.

Structure analysis by electron crystallography. The methodological approach for structure analysis is briefly outlined below; details are reviewed elsewhere (2).

Generally the optimization of conditions for 2-D crystal growth is carried out by negative-stain electron microscopy. The specimen, after settling on a carbon film overlaying an electron microscope grid, is embedded in a heavy metal salt such as uranyl acetate or sodium phosphotungstate and then viewed in an electron microscope. The presence of crystalline areas, the degree of order, and the extent of the coherent areas are judged by examination of recorded images in an optical diffractometer. Embedding the sample in a heavy metal salt stain produces a surface relief so that only lowresolution information (generally greater than \sim 18 A) is obtainable. Analysis of negatively stained crystals in projection, albeit at low resolution, is very useful for rapid determination of crystal symmetry, lattice dimensions, and overall molecular shape and oligomeric state. However, no information about the structure in the bilayer can be derived, because the polar heavy metal stain does not significantly permeate the hydrophobic lipid bilayer. The alternate approaches of embedding in sugar such as glucose (37), trehalose (52), and tannin (54) or preserving in a frozen-hydrated state in vitrified buffer (3, 98, 123) are required for achieving higher resolution and visualizing the full 3-D structure. Typically, the analysis is first carried out in projection using data derived from electron micrographs of crystals viewed in the direction of the electron beam. Areas of recorded images that diffract to the highest resolution in an optical diffractometer are digitized and then Fourier transformed in a computer. The amplitudes and phases of the Fourier components are extracted after application of algorithms (e.g., suite of programs from the Medical Research Council in Cambridge, Ref. 43) that correct for lattice distortion and the effects of lens defocus. Inverse Fourier transformation of the amplitudes and phases then yields a map of the protein density viewed in a direction perpendicular to the plane of the bilayer. To determine the structure in three dimensions, the specimen is tilted with respect to the electron beam, and multiple 2-D projected views are recorded. The data from the tilted views are analyzed computationally to generate a 3-D density map.

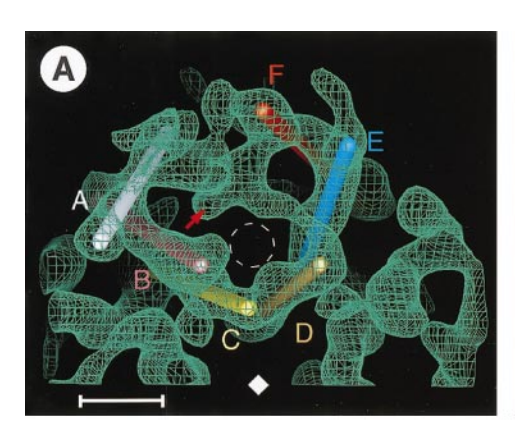
History of electron crystallography of AQP1. The ease of generating milligram quantities of purified AQP1 from erythrocytes has facilitated structural analysis. 2-D crystals of AQP1 were generated by three groups using different conditions for crystallization. These crystals were subjected to electron cryocrystallographic analyses to determine the structure in projection (46, 75, 112) using different methods for specimen preservation. Walz et al. (112) used samples of glucoseembedded, native, partially glycosylated AQP1 from human erythrocytes crystallized in lipids extracted from *E. coli*. Glucose embedding was also employed by Jap and Li (46) using native, bovine AQP1 (earlier called CHIP29) crystallized in dimyristoyl phosphatidylcholine (DMPC). We crystallized deglycosylated, human erythrocyte AQP1 in dioleoyl phosphatidylcholine (DOPC) bilayers and examined frozen-hydrated crystals in vitrified buffer without stain (75). Notwithstanding these differences in the conditions of crystallization

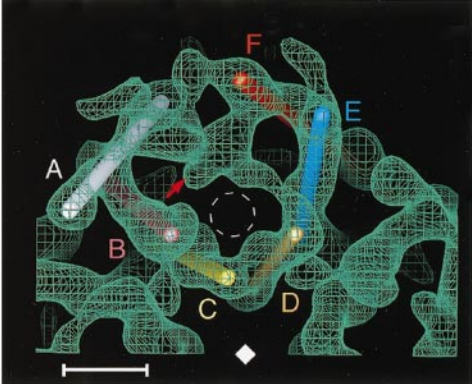
and specimen preparation, the three projection maps revealed overall similarities: tetrameric packing of the AQP1 monomers and multiple density peaks in each monomer suggestive of α -helical segments.

Subsequently, we reported the unperturbed 7-A resolution 3-D structure of frozen-hydrated AQP1 determined by analysis of minimal dose images and electrondiffraction patterns recorded from 2-D crystals tilted up to 45° (15). Similar 3-D density maps were reported by the other two groups (64, 109), which were determined using specimens preserved in trehalose with the tilted projections comprising images and electron diffraction patterns (109) or only images (64). All three maps reveal a barrel formed by six helices surrounding additional density; the helices pack with a righthanded twist in the models of Cheng et al. (15) and Walz et al. (109) but with a left-handed twist in the model of Li et al. (64). The 3-D models of Walz et al. (109) and Cheng et al. (15) indicated an asymmetric disposition of AQP1 in the bilayer consistent with results from atomic force microscopy (AFM) (111) that indicated larger extrabilayer mass on the cytoplasmic face of AQP1. Walz et al. (109) suggested a possible positional assignment of the six helices based on their AFM results (111) and attribution of some of the density features in the 3-D map to interhelix loops.

Interpretation of 3-D density map obtained from frozen-hydrated AQP1 crystals. To date, all structural studies at atomic or near-atomic resolution using electron crystallography have made use of crystalline samples in sugars. However, frozen-hydrated specimens in vitreous ice offer potential advantages in maintaining native protein environment (99). Also, at least in one case, purple membrane, the structure of an intermediate state directly involved in protein functioning, was found to be altered upon preservation in sugar (36, 92).

Figure 3A shows that four AQP1 monomers are arranged symmetrically around a fourfold axis oriented perpendicular to the bilayer. The overall density for each monomer is approximately cylindrical ($\sim\!30~\text{Å}$ diameter and $\sim\!60~\text{Å}$ height). The prominent feature in a monomer is a barrel formed by six, approximately cylindrical, tilted (18–30 Å) rods of density (A-F, $\sim\!36$ –44 Å length) representing the six TM α -helices. All six helices show some degree of curvature, especially helix D on the cytoplasmic side and helix F, which displays a distinct kink and could be thought of as being composed of two short helices. The bends in the helices could be due to the presence of several glycine and/or proline residues located within the putative membrane-spanning regions of the polypeptide chain. Within a mono-





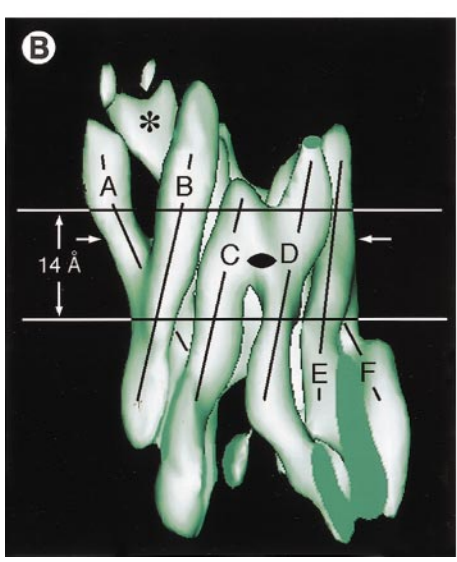


Fig. 3. Electron crystallography of AQP1 crystals in reconstituted proteoliposomes. A: stereo pair of three-dimensional (3-D) density maps of frozenhydrated AQP1 viewed approximately perpendicular to the bilayer. The rods trace the approximate paths of the centers of 6 tilted helices packed with a right-handed twist. These helices surround a vestibular region that narrows to a diameter of ~8 Å (indicated by dashed circle in the center). Arrow indicates density assigned to the vertically apposed NPA sequences. B: surfaceshaded representation of the 6-helix barrel viewed parallel to the bilayer. In-plane molecular pseudo twofold symmetry (black ellipse) is strongest within the demarcated transmembrane region. Asterisk indicates a portion of density bridging density attributed to NPA box to helix F. Reprinted by permission from Nature [Cheng et al. (15)], copyright 1997, Macmillan Magazines, Ltd.

F22 INVITED REVIEW

mer, interactions among the six helices are elaborated in three tightly packed two-helix bundles. Also, near the fourfold axis, interactions that may contribute to the stability of a tetramer are suggested by strong overlap of density between helices B, C and D, E belonging to adjacent monomers. In contrast, helices A and F delineate a comparatively more open, membraneembedded face of the molecule as noted also by Li et al. (64) in their 3-D density map of bovine AQP1. The six-helix barrel encloses a central block of density that appears to be linked to the surrounding protein barrel. Two sets of bridges of density suggest linkages of this central block to the surrounding barrel. One, located on the proximal side as viewed in Fig. 3B, is directed toward helices F and D, and the other, located on the distal side, is directed toward helices A and C. These bridges and the block of density reside within the interior of the protein and have been attributed to predominantly hydrophobic segments containing the conserved NPA sequences in loops connecting the second and third and the fifth and sixth helices on the opposite sides of the bilayer (15, 64, 109).

The 3-D structure of AQP1 shows evidence of an internal symmetry related to the homology of the first and second halves of the aquaporin amino acid sequence discussed above. Examination of our 3-D density map revealed a symmetric disposition of protein density in the hydrophobic core of each AQP1 monomer. Thus planes of 3-D density, parallel to the bilayer and equidistant above and below a particular plane (located \sim 3 A toward the extracellular side from the center of mass), can be superposed by a 180° rotation around an axis inclined by $\sim 10^{\circ}$ to a lattice edge. This (2-fold) "pseudo-symmetry" is strongest within a span of ${\sim}14~\mathrm{A}$ near the center of an AQP1 molecule (Fig. 3B). In membrane proteins, intramolecular pseudo-symmetry has been seen in LHC II (54) between two homologous helices where the twofold axis is oriented perpendicular to the membrane plane. The twofold symmetry in the membrane plane and the tandem repeats in the AQP1 sequence might provide a simple explanation for bidirectional water transport through aquaporins.

As described above, existing lines of evidence suggest that each AQP1 monomer encloses a functional channel. Examination of the 3-D density map reveals that within a monomer and near the fourfold axis, a region of low, continuous protein density delineates a vestibular region that is outlined by the density attributed to the polypeptide chain neighboring the NPA regions. This low-density region narrows down to ~8 Å in diameter near the center of the bilayer and likely encloses the channel (Fig. 3A). Recent high-resolution analysis in projection of 2-D AQP1 crystals labeled with the channel blocker *para*-chloromercuribenzenesulfonate (pCMBS) (85) is consistent with this location for the channel. The indicated dimension is too large to explain selectivity for water; however, positioning of the side chains that should be visible in a higher resolution map may result in an appropriate dimension $(\sim 3.2 \text{ A})$ for the putative channel. The current resolution of AQP1 structure is too low to assign amino acid locations. On the basis of the low activation energy for water transport, we speculate that a set of polar and/or charged residues present in the transmembrane segments constitutes the lining of the narrow hydrated pore.

Model for AQP1 topology. Although the current resolution of the map (7 A in plane and \sim 18 A perpendicular to the bilayer) does not allow unique positional assignment of helices, we note several features that restrict the number of possible models of AQP1 topology. The in-plane twofold symmetry and the tandem repeat motif of AQP1 restrict the positional assignment of homologous helical segments (helices 1 and 4, 2 and 5, and 3 and 6). In addition, helix assignment is further restricted by the identification of the cytoplasmic face of the molecule with larger extrabilayer mass and the putative linkages to the central "NPA" density identifying helices 2 and 3, or 5 and 6. Combining these constraints, Fig. 4 shows a working model for the AQP1 topology in which helix position and orientation are specified (see legend to Fig. 4). This model is also consistent with the location of the mercurial binding

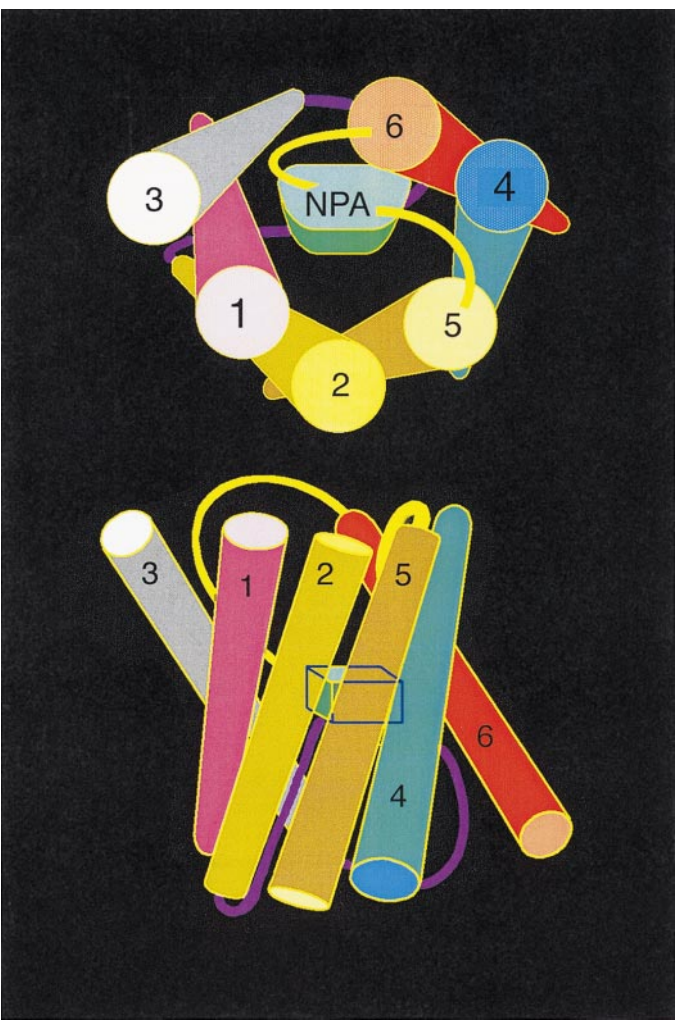


Fig. 4. Schematic representation of a possible topology model for the arrangement of membrane-spanning helical segments in AQP1. Model is based on deductions made from our 7-Å 3-D density map (15).

site (85) near the putative channel indicated in Fig. 3*A*. Validation or correction of this helix assignment must await an atomic resolution structure.

CELLULAR BIOGENESIS OF AQUAPORINS

The folding and assembly of polytopic membrane proteins occur in the rough endoplasmic reticulum (ER), where TM helices and cytosolic and extracytosolic peptide loops are properly oriented relative to the membrane by a series of protein translocation events. Despite their similar predicted structures and functional properties, different aquaporins appear to utilize markedly different folding pathways to acquire their final topology (88, 91). For AQP4, each of its six TM helices is cotranslationally and sequentially inserted into the ER membrane as the nascent polypeptide emerges from the ribosome (88). During this process, translocation is initiated and terminated by alternating independent internal signal and stop transfer sequence encoded within the nascent chain. In contrast, AQP1 utilizes a more complex folding pathway that involves at least three identifiable folding intermediates (66). First, cotranslational translocation events establish an initial AQP1 topology with only four TM segments (TM2 and TM4 are initially positioned on luminal and cytosolic faces of the membrane, respectively) (91). Second, this four-spanning structure undergoes a topological reorientation in which TM3 rotates 180° from a type I to a type II topology, resulting in reorientation of TM2 and TM4. Third, AQP1 undergoes additional compaction to acquire a mature proteaseresistant core structure. Detailed examination of AQP1/ AQP4 chimeras has recently identified residues at the NH₂ terminus of TM2 and the COOH terminus of TM3 that give rise to these different folding pathways by altering the topogenic properties of signal and stop transfer sequences (33). In the case of TM2, residues N49 and K51 in AQP1 are replaced by M48 and L50 in AQP4. As a result, AQP1-TM2 is less hydrophobic and thus probably shorter than AQP1-TM2. This could result in inability of TM2 to independently terminate translocation and span the membrane. Interestingly, residues N49 and K51 are also required for AQP1 function as determined by mutagenesis studies in *Xenopus* oocytes. The unexpected level of complexity of AQP1 biogenesis makes it a useful tool to establish new paradigms in polytopic membrane protein biogenesis, such as that related to topogenic reorientation.

AQUAPORIN MEMBRANE DIFFUSION AS A NOVEL PROBE OF PORE STRUCTURE

Spectroscopic and crystallographic analyses of a protein in the bilayer generally provide static information about conformation. For channel proteins, functional transport measurements provide a dynamic probe of pore structure giving information about pore geometry and pore surface-water interactions. To generate a mechanistic picture of channel function, such information is used in conjunction with molecular dynamics simulations on an atomic resolution structure, which is unavailable at present. We propose that measurement

of flow-induced changes in aquaporin mobility might provide an independent, more readily interpretable probe of aquaporin pore structure. As water flows through a pore, changes in flow direction impart a momentum that is in principal observable as a flow-dependent displacement of the channel. This mechanism is responsible for the flow-driven rotation of a garden sprinkler in which the heads redirect the initially vertical water flow.

To establish a strategy to measure flow-dependent changes in aquaporin membrane mobility, a series of GFP-aquaporin chimeras were constructed and analyzed (Fig. 5A) (97). In transfected mammalian cells, the GFP moiety did not affect aquaporin function, tetrameric association, or plasma membrane targeting. GFP-aquaporin membrane mobility was measured by fluorescence recovery after photobleaching, in which a spot on the cell membrane is irreversibly bleached by a brief intense laser beam. The recovery of fluorescence into the bleached region provides a quantitative measure of fluorophore lateral mobility. Figure 5*B* shows the fluorescence recovery of GFP-AQP1 in transfected LLC-PK₁ cells. Unbleached fluorophore moved slowly into the bleach region; quantitative analysis by spot photobleaching (Fig. 5*C*) showed that GFP-AQP1 was freely diffusible in the plane of the membrane with a diffusion coefficient of 10^{-10} cm²/s. Similar experiments were performed just after an osmotic gradient was applied to induce water flow through the pore. Water flow did not affect the apparent GFP-AQP1 diffusion coefficient (unpublished results). This is consistent with the fact that adjacent AQP1 monomers in each tetramer are rotated by 90°, imparting zero net linear momentum. A flow-induced change in aquaporin mobility is predicted to induce a change in aquaporin rotation rather than in translation. The challenge will be to develop the biophysical methodology to quantify microsecond aquaporin rotations. This will require the construction of rigid GFP-aquaporin chimeras that do not undergo submicrosecond depolarizing rotations, as well as the adaptation of polarization photobleaching recovery or fluorescence correlation spectroscopy methods.

AQUAPORINS AS TARGETS FOR DRUG DISCOVERY

It was reported in 1994 that mutations in the AQP2 water channel cause the very rare non-X-linked form of hereditary nephrogenic diabetes insipidus (21). More than 25 mutations in human AQP2 have been reported to date, including null mutations, mutations that result in AQP2 retention at the ER (19, 94), and a dominant mutation resulting in AQP2 retention at the Golgi (51). Clearly AQP2 is required for production of a concentrated urine by the kidney. The only other aquaporin for which natural mutations are known is AQP1, in which three exceedingly rare individuals were identified on the basis of their Colton null blood group (83). These individuals were reported to be phenotypically normal despite having low erythrocyte water permeability; however, these individuals were not subject to any clinical evaluation. Therefore, the physiological significance of aquaporins other than AQP2 was uncertain.

F24 INVITED REVIEW

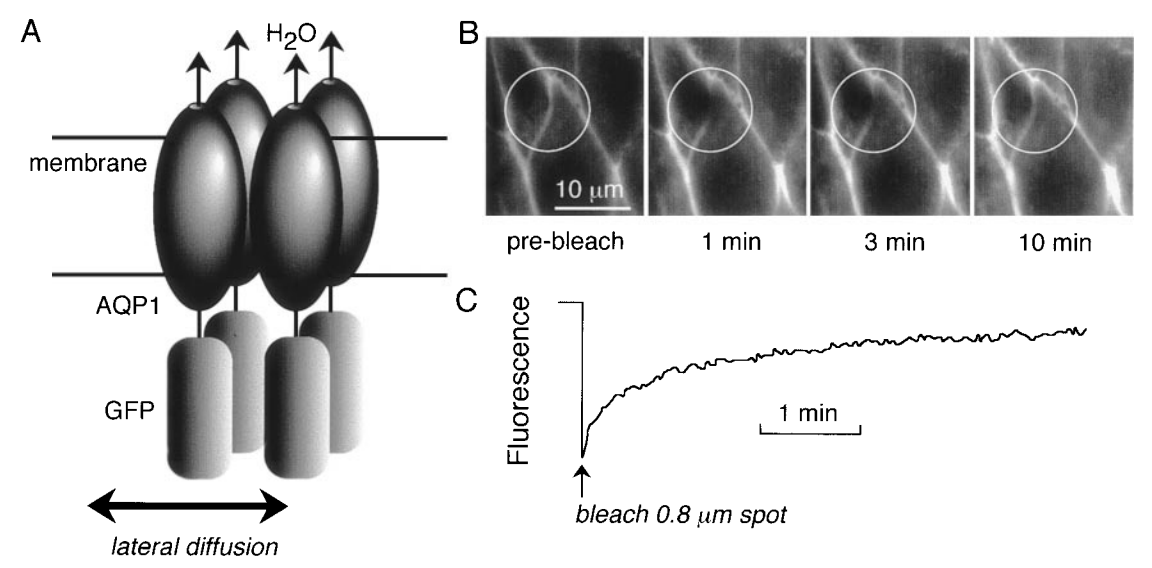


Fig. 5. Aquaporin mobility in membranes studied by fluorescence recovery after photobleaching. LLC-PK $_1$ cells were stably transfected with a GFP-AQP1 chimera containing the green fluorescent protein (GFP) at the AQP1 NH $_2$ terminus. A: cartoon showing GFP-AQP1 tetramer in a membrane in which each AQP1 monomer labeled with a GFP molecule. B: GFP fluorescence of transfected LLC-PK $_1$ cells showing a membrane expression pattern. Fluorescence was bleached by a brief, intense laser beam within the area demarcated by the white circle. Images shown before bleach (prebleach) and at indicated times after bleach. C: recovery curve measured using a 0.8- μ m-diameter focused laser spot. See text for further explanations.

To define the roles of aquaporins and thus evaluate their suitability as targets for drug discovery, our laboratory has generated transgenic aquaporin knockout mice by targeted gene disruption. To date, we have generated null mice lacking AQP1, AQP3, AQP4, AQP5, and AQP8. For detailed phenotype descriptions the reader is referred to recent reviews (69, 70, 106, 107) and the original studies cited therein. In brief, multiple phenotype abnormalities were found such as defective urinary concentrating ability in AQP1 and AQP3 null mice, defective saliva production in AQP5 null mice, altered cerebral water balance in AQP4 null mice, defective dietary fat processing in AQP1 null mice, and very low lung water permeability in AQP1 and AQP5 null mice. However, the expression of an aquaporin in a tissue does not ensure a demonstrable physiological role. For example, despite AQP4 expression in gastric parietal cells and skeletal muscle plasmalemma, no impairments in gastric acidification and muscle function were found in AQP4 null mice.

From these considerations, we propose that aquaporin blockers might have clinical applications as aquaretics in hypertension and congestive heart failure, inhibitors of brain swelling following head trauma or stroke, modulators of pulmonary edema, and regulators of increased intracranial and intraocular pressure. Aquaporin activators or aquaporin gene replacement might be useful in glandular hypofunction such as in Sjogren's syndrome and in water diuretic states. The only known compounds that inhibit water/solute transport in some of the aquaporins are mercurial sulfhydryl-reactive compounds, which are nonspecific cysteine-binding reagents that are too toxic for in vivo use. Two potentially useful strategies to identify pharmacologically useful aquaporin modulators include structure-based drug

design and high-throughput screening of combinatorial drug libraries. An atomic resolution structure, unavailable as of now, is required to initiate experiments directed at de novo drug design. High-throughput screening of a library of small drug-like compounds is in progress (93) utilizing suitable transfected cells models and automated quantitative assays of cell water permeability. The compounds identified by high-throughput screening may be useful in probing aquaporin pore structure and studying animal physiology and potentially in the treatment of human disease.

PERSPECTIVE AND DIRECTIONS

Although research in aquaporin structure and function has advanced rapidly in part because of the relative ease of aquaporin purification (in the case of AQP1), 2-D crystallization, mutagenesis, and functional analysis, there remain major unresolved issues. Little is known about intramolecular dynamics in aquaporin proteins; it is not known whether aquaporins undergo conformational changes or gating. Improved resolution in electron crystallographic analysis of AQP1 structure and/or high-resolution X-ray crystallography will be needed to unambiguously identify the water pathway. Purification and crystallographic analysis of other aquaporins is needed, particularly the aquaglyceroporins, to identify the small solute pathway, as well as to test whether all aquaporins have similar basic structure and to determine differences in structure that may be related to solute specificity. As nonmercurial water channel inhibitors are identified, structural analysis may provide key information about inhibition mechanisms and facilitate the engineering of compounds with greater inhibitory potencies.

There remain many questions about aquaporin function. The possibility that aquaporins transport small gases and other solutes requires further investigation because of its physiological relevance, as does the possibility that intrinsic aquaporin function may be subject to biochemical regulation. From an organismal perspective, the role of aquaporin-mediated small solute transport remains unknown. Although phenotype studies on transgenic mouse models have defined the water-transporting role of aquaporins in several organ systems, much remains to be done in defining the role of aquaporins in gastrointestinal, neuromuscular, eye, and reproductive function. The possibility that aquaporins participate in functions that do not involve membrane transport warrants consideration. The high membrane density and very hydrophobic nature of aquaporins and the regular intramembrane assembly of AQP4 suggest a possible role in membrane fluidity and possibly structural integrity. The identification of AQP1 as an early response gene to mitogens (62) and preliminary evidence showing AQP1 expression in tumor microvessels and reduced tumor growth and angiogenesis in AQP1-deficient mice raise the possibility that aquaporins may be involved in tumor growth and angiogenesis (unpublished results). Last, investigation is needed to identify functionally significant interactions between aquaporins and other membrane and cytoplasmic proteins.

This work was supported by National Institutes of Health (NIH) Grants DK-35124, HL-51854, HL-42368, and DK-43840 and National Cystic Fibrosis Foundation Grant R613 (to A. S. Verkman) and NIH Grant GM-52567 and a Grant-in-Aid from the American Heart Association (to A. K. Mitra).

Address for reprint requests and other correspondence: A. S. Verkman, 1246 Health Sciences East Tower, Cardiovascular Research Institute, Univ. of California, San Francisco, San Francisco, CA 94143-0521 (E-mail: verkman@itsa.ucsf.edu) (website: http://www.ucsf.edu/verklab).

REFERENCES

- Agre, P., M. D. Lee, S. Devidas, and W. B. Guggino. Aquaporins and ion conductance. *Science* 275: 1490, 1997.
- Amos, L. A., R. Henderson, and P. N. T. Unwin. Threedimensional structure determination by electron microscopy of two-dimensional crystals. *Prog. Biophys. Mol. Biol.* 39: 183– 231, 1982.
- 3. **Auer, M., G. A. Scarborough, and W. Kuhlbrandt.** Three-dimensional map of the plasma membrane H⁺-ATPase in the open conformation. *Nature* 392: 840–843, 1998.
- Bai, L., K. Fushimi, S. Sasaki, and F. Marumo. Structure of aquaporin-2 vasopressin water channel. *J. Biol. Chem.* 271: 5171–5176, 1996.
- Baumgarten, R., M. H. van de Pol, J. F. Wetzels, C. H. van Os, and P. M. Deen. Glycosylation is not essential for vasopressin-dependent routing of aquaporin-2 in transfected Madin-Darby canine kidney cells. J. Am. Soc. Nephrol. 9: 1553–1559, 1998
- Berriman, J., and N. Unwin. Analysis of transient structures by cryo-microscopy combined with rapid mixing of spray droplets. *Ultramicroscopy* 56: 241–252, 1994.
- Bicknese, S., J. Park, D. Zimet, A. N. van Hoek, S. B. Shohet, and A. S. Verkman. Detection of water proximity to tryptophan residues in proteins by single photon radioluminescence. *Biophys. Chem.* 54: 279–290, 1995.
- Bicknese, S., Z. Shahrohk, S. B. Shohet, and A. S. Verkman. Single photon radioluminescence. I. Theory and spectroscopic properties. *Biophys. J.* 63: 1256–1266, 1992.

 Borgnia, M. J., D. Kozono, P. Maloney, and P. Agre. Purification and functional reconstitution of bacterial aquaporins (Abstract). *Biophys. J.* 76: 436, 1999.

- Buchanan, S. K., B. S. Smith, L. Venkatramani, D. Xia, L. Esser, M. Palnitkar, R. Chakraborty, D. van der Helm, and J. Deisenhofer. Crystal structure of the outer membrane active transporter FepA from *Escherichia coli*. Nat. Struct. Biol. 6: 56–63, 1999.
- Cabiaux, V., K. A. Oberg, P. Pancoska, T. Walz, P. Agre, and A. Engel. Secondary structures comparison of aquaporin-1 and bacteriorhodopsin: a Fourier transform infrared spectroscopy study of two-dimensional membrane crystals. *Biophys. J.* 73: 406–417, 1997.
- Cahalan, K. L., and J. E. Hall. pH sensitivity of MIP-induced water permeability may play a role in regulating the intrinsic fluid circulation of the lens (Abstract). *Biophys. J.* 76: 183, 1999.
- Chang, G., R. H. Spencer, A. T. Lee, M. T. Barclay, and D. C. Rees. Structure of the MscL homolog from *Mycobacterium* tuberculosis: a gated mechanosensitive ion channel. *Science* 82: 2220–2226, 1998.
- Chandy, G., G. A. Zampighi, M. Kreman, and J. E. Hall. Comparison of the water transporting properties of MIP and AQP1. *J. Membr. Biol.* 159: 29–39, 1997.
- Cheng, A., A. N. van Hoek, M. Yaeger, A. S. Verkman, and A. K. Mitra. Three-dimensional organization of a human water channel. *Nature* 387: 627–630, 1997.
- Chou, C. L., M. A. Knepper, A. N. van Hoek, D. Brown, B. Yang, T. Ma, and A. S. Verkman. Reduced water permeability and altered ultrastructure in thin descending limb of Henle in aquaporin-1 null mice. *J. Clin. Invest.* 103: 491–496, 1999.
- Cooper, G. J., and W. F. Boron. Effect of PCMBS on CO₂ permeability of *Xenopus* oocytes expressing aquaporin 1 or its C189S mutant. *Am. J. Physiol. Cell Physiol.* 275: C1481–C1486, 1998.
- Coury, L. A., J. C. Mathai, G. V. Prasad, J. L. Brodsky, P. Agre, and M. L. Zeidel. Reconstitution of water channel function of aquaporins 1 and 2 by expression in yeast secretory vesicles. *Am. J. Physiol. Renal Physiol.* 274: F34–F42, 1998.
- 19. Deen, P. M., H. Croes, R. A. van Aubel, L. A. Ginsel, and C. H. van Os. Water channels encoded by mutant aquaporin-2 genes in nephrogenic diabetes insipidus are impaired in their cellular routing. *J. Clin. Invest.* 9: 2291–2296, 1995.
- Deen, P. M., S. M. Mulders, S. M. Kansen, and C. H. van Os. Aquaporins and ion conductance. *Science* 275: 1491, 1997.
- Deen, P. M., M. A. Verkijk, N. V. Knoers, B. Wieringa, L. A. Monnens, C. H. van Os, and B. A. van Oost. Requirement of human renal water channel aquaporin-2 for vasopressindependent concentration of urine. *Science* 264: 92–95, 1994.
- 22. Doyle, D. A., J. M. Cabral, R. A. Pfuetzner, A. Kuo, J. M. Gulbis, S. L. Cohen, B. T. Chait, and R. MacKinnon. The structure of the potassium channel: molecular basis of K⁺ conduction and selectivity. *Science* 280: 69–77, 1998.
- Echevarria, M., E. E. Windhager, and G. Frindt. Selectivity
 of the renal collecting water channel aquaporin-3. *J. Biol. Chem.* 271: 25079–25082, 1996.
- 24. Echevarria, M., E. E. Windhager, S. S. Tate, and G. Frindt. Cloning and expression of AQP3, a water channel from the medullary collecting duct of rat kidney. *Proc. Natl. Acad. Sci.* USA 91: 10997–11001, 1994.
- 25. Farinas, J., M. Kneen, M. Moore, and A. S. Verkman. Plasma membrane water permeability of cultured cells and epithelia measured by light microscopy with spatial filtering. *J. Gen. Physiol.* 110: 283–296, 1997.
- 26. Farinas, J., V. Simenak, and A. S. Verkman. Cell volume measured in adherent cells by total internal reflection microfluorimetry: application to permeability in cells transfected with water channel homologs. *Biophys. J.* 68: 1613–1620, 1995.
- 27. Farinas, J., A. N. van Hoek, L. B. Shi, C. Erickson, and A. S. Verkman. Non-polar environment of tryptophans in erythrocyte water channel CHIP28 determined by fluorescence quenching. *Biochemistry* 32: 11857–11864, 1993.
- Farinas, J., and A. S. Verkman. Fluorescence depolarization of fluorescein-labeled erythrocyte water channel CHIP28 (Abstract). *Biophys. J.* 66: 166, 1994.

F26 INVITED REVIEW

 Farinas, J., and A. S. Verkman. Measurement of cell volume and water permeability in epithelial cell layers by interferometry. *Biophys. J.* 71: 3511–3522, 1996.

- Ferguson, A. D., E. Hofmann, J. W. Coulton, K. Diederichs, and W. Welte. Siderophore-mediated iron transport: crystal structure of FhuA with bound lipopolysaccharide. *Science* 282: 2215–2220, 1998.
- Finkelstein, A. Water Movement Through Lipid Bilayers, Pores, and Plasma Membranes: Theory and Reality. New York: Wiley, 1987.
- Fischbarg, J., K. Kunyan, J. C. Vera, S. Arant, S. Silverstein, J. Loike, and O. M. Rosen. Glucose transporters serve as water channels. *Proc. Natl. Acad. Sci. USA* 87: 3244–3247, 1990
- 33. Foster, W., A. Helm, Y. Lu, A. S. Verkman, W. R. Skach. Identification of sequence determinants responsible for different intracellular folding pathways of AQP1 and AQP4 (Abstract). J. Am. Soc. Nephrol. 9: 128, 1998.
- 34. Frigeri, A., M. Gropper, F. Umenishi, M. Kawashima, D. Brown, and A. S. Verkman. Localization of MIWC and GLIP water channel homologs in neuromuscular, epithelial and glandular tissues. J. Cell Sci. 108: 2993–3002, 1995.
- Fushimi, K., S. Uchida, Y. Hara, Y. Hirata, F. Marumo, and S. Sasaki. Cloning and expression of apical membrane water channel of rat kidney collecting tubule. *Nature* 361: 549–552, 1993.
- Glaeser, R. M., J. Baldwin, T. A. Ceska, and R. Henderson. Electron diffraction analysis of the M412 intermediate of bacteriorhodopsin. *Biophys. J.* 50: 913–920, 1986.
- Grigorieff, N., T. A. Ceska, K. H. Downing, J. M. Baldwin, and R. Henderson. Electron-crystallographic refinement of the structure of bacteriorhodopsin. *J. Mol. Biol.* 259: 393–421, 1996.
- 38. **Han, Z., M. B. Wax, and P. V. Patil.** Regulation of aquaporin-4 water channels by phorbol ester-dependent protein phosphorylation. *J. Biol. Chem.* 273: 6001–6004, 1998.
- Haris, P. I., D. Chapman, and G. Benga. A Fourier-transform infrared spectroscopy investigation of the hydrogen-deuterium exchange and secondary structure of the 28-kDa channelforming integral membrane protein (CHIP28). Eur. J. Biochem. 233: 659–664, 1995.
- Hasegawa, H., T. Ma, W. Skach, M. Matthay, and A. S. Verkman. Molecular cloning of a mercurial-insensitive water channel expressed in selected water transporting tissues. *J. Biol. Chem.* 269: 5497–5500, 1994.
- Hasegawa, H., W. Skach, O. Baker, M. C. Calayag, V. Lingappa, and A. S. Verkman. A multi-functional aqueous channel formed by CFTR. *Science* 258: 1477–1479, 1992.
- Hasler, L., J. B. Heymann, A. Engel, J. Kistler, and T. Walz.
 crystallization of membrane proteins: rationales and examples. J. Struct. Biol. 121: 162–171, 1998.
- Henderson, R., J. M. Baldwin, T. A. Ceska, F. Zemlin, E. Beckmann, and K. H. Downing. Model for the structure of bacteriorhodopsin based on high-resolution electron cryomicroscopy. *J. Mol. Biol.* 213: 899–929, 1990.
- 44. Ishibashi, K., M. Kuwahara, Y. Gu, Y. Kageyama, A. Tohsaka, F. Suzuki, F. Marumo, and S. Sasaki. Cloning and functional expression of a new water channel abundantly expressed in the testis permeable to water, glycerol and urea. *J. Biol. Chem.* 272: 20782–20786, 1997.
- 45. Ishibashi, K., S. Sasaki, K. Fushimi, S. Uchida, M. Kuwahara, H. Saito, T. Furukawa, K. Nakajima, Y. Yamaguchi, T. Gojobori, and F. Marumo. Molecular cloning and expression of a member of the aquaporin family with permeability to glycerol and urea in addition to water expressed at the basolateral membrane of kidney collecting duct cells. *Proc. Natl. Acad. Sci. USA* 91: 6269–6273, 1994.
- Jap, B. K., and H. Li. Structure of the osmoregulated H₂O-channel, AQP-CHIP, in projection at 3.5 Å resolution. *J. Mol. Biol.* 251: 413–420, 1995.
- Jap, B. K., M. Zulauf, T. Scheybani, A. Hefti, W. Baumeister, U. Aebi, and A. Engel. 2D crystallization: from art to science. *Ultramicroscopy* 46: 45–84, 1992.

- Jiang, J. X., and D. A. Goodenough. Heteromeric connexons in lens gap junction channels. *Proc. Natl. Acad. Sci. USA* 93: 1287–1291, 1996.
- Johansson, I., M. Karlsson, V. K. Skukla, M. J. Chrispeels,
 C. Larsson, and P. Kjellbom. Water transport activity of the plasma membrane aquaporin PM28A is regulated by phosphorylation. *Plant Cell* 10: 451–459, 1998.
- Jung, J. S., G. M. Preston, B. L. Smith, W. B. Guggino, and P. Agre. Molecular structure of the water channel through aquaporin CHIP. The hourglass model. *J. Biol. Chem.* 269: 14648–14654, 1994.
- Kamsteeg, E. J., T. A. Wormhoudt, J. P. Rijss, C. H. van Os, and P. M. Deen. An impaired routing of wildtype aquaporin-2 after tetramerization with an aquaporin-2 mutant explains dominant nephrogenic diabetes insipidus. *EMBO J.* 18: 2394– 2400, 1999.
- 52. Kimura, Y., D. G. Vassylyev, A. Miyazawa, A. Kidera, M. Matsushima, K. Mitsuoka, K. Murata, T. Hirai, and Y. Fujiyoshi. Surface of bacteriorhodopsin revealed by high-resolution electron crystallography. *Nature* 389: 206–211, 1997.
- Kuhlbrandt, W. Two-dimensional crystallization of membrane proteins. Q. Rev. Biophys. 25: 1–49, 1992.
- 54. Kuhlbrandt, W., D. N. Wang, and Y. Fujiyoshi. Atomic model of plant light-harvesting complex by electron crystallography. *Nature* 367: 614–621, 1994.
- 55. Kuwahara, M., K. Fushimi, Y. Terada, L. Bai, F. Marumo, and S. Sasaki. cAMP-dependent phosphorylation stimulates water permeability of aquaporin-collecting duct water channel protein expressed in *Xenopus* oocytes. *J. Biol. Chem.* 270: 10384–10387.
- 56. Kuwahara, M., Y. Gu, K. Ishibashi, F. Marumo, and S. Sasaki. Mercury-sensitive residues and pore site in AQP3 water channel. *Biochemistry* 36: 13973–13978, 1997.
- 57. Lagree, V., A. Froger, S. Deschamps, J. F. Hubert, C. Delamarche, G. Bonnec, D. Thomas, J. Gouranton, and I. Pellerin. Switch from an aquaporin to a glycerol channel by two amino acids substitution. J. Biol. Chem. 274: 6817–6719, 1999.
- Lagree, V., A. Froger, S. Deschamps, I. Pellerin, C. Delamarche, G. Bonnec, J. Gouranton, D. Thomas, and J. F. Hubert. Oligomerization state of water channels and glycerol facilitators. Involvement of loop E. J. Biol. Chem. 273: 33949–33953, 1998.
- 59. Lagree, V., I. Pellerin, J. F. Hubert, F. Tacnet, F. Le Caherec, N. Roudier, D. Thomas, J. Gouranton, and S. Deschamps. A yeast recombinant aquaporin mutant that is not expressed or mistargeted in *Xenopus* oocyte can be functionally analyzed in reconstituted proteoliposomes. *J. Biol. Chem.* 273: 12422–12426, 1998.
- Laize, V., P. Ripoche, and F. Tacnet. Purification and functional reconstitution of the human CHIP28 water channel expressed in *Saccharomyces cerevisiae*. Protein Expr. Purif. 11: 284–288, 1997.
- 61. Laize, V., G. Rousselet, J. M. Verbavatz, V. Berthonaud, R. Gobin, N. Roudier, L. Abrami, P. Ripoche, and F. Tacnet. Functional expression of the human CHIP28 water channel in a yeast secretory mutant. FEBS Lett. 373: 269–274, 1995.
- Lanahan, A., J. B. Williams, L. K. Landers, and D. Nathans. Growth factor-induced delayed early response genes. *Mol. Cell. Biol.* 12: 3919–3929, 1992.
- 63. Lande, M. B., I. Jo, M. L. Zeidel, M. Somers, and H. W. Harris. Phosphorylation of aquaporin-2 does not alter the membrane water permeability of rat papillary water channel-containing vesicles. *J. Biol. Chem.* 271: 5552–5557, 1996.
- 64. **Li, H., S. Lee, and B. K. Jap.** Molecular design of aquaporin-1 water channel as revealed by electron crystallography. *Nat. Struct. Biol.* 4: 263–265, 1997.
- Loo, D. D., B. A. Hirayama, A. K. Meinild, G. Chandy, T. Zeuthen, and E. M. Wright. Passive water and ion transport by cotransporter. *J. Physiol.* 518: 195–202, 1999.
- 66. Lu, Y., A. S. Verkman, and W. R. Skach. Topological reorientation of AQP1 at the ER membrane (Abstract). *Mol. Biol. Cell* 9, *Suppl.*: 2011, 1998.

- 67. **Ma, T., A. Frigeri, H. Hasegawa, and A. S. Verkman.** Cloning of a water channel homolog expressed in brain meningeal cells and kidney collecting duct that functions as a stilbenesensitive glycerol transporter. *J. Biol. Chem.* 269: 21845–21849, 1994.
- 68. Ma, T., A. Frigeri, S. T. Tsai, J. M. Verbavatz, and A. S. Verkman. Localization and functional analysis of CHIP28k water channels in stably transfected CHO cells. *J. Biol. Chem.* 268: 22756–22764. 1993.
- 69. Ma, T., Y. Song, A. Gillespie, E. J. Carlson, C. J. Epstein, and A. S. Verkman. Defective secretion of saliva in transgenic mice lacking aquaporin-5 water channels. *J. Biol. Chem.* 274: 20071–20071, 1999.
- 70. **Ma, T., and A. S. Verkman.** Aquaporin water channels in gastrointestinal physiology. *J. Physiol.* 517: 317–326, 1999.
- Marinelli, R. A., P. S. Tietz, L. D. Pham, L. Rueckert, P. Agre, and N. F. LaRusso. Secretin induced the apical insertion of aquaporin-1 water channels in rat cholangiocytes. *Am. J. Physiol. Gastrointest. Liver Physiol.* 276: G280–G286, 1999.
- Marples, D., J. Frokiaer, and S. Nielsen. Long-term regulation of aquaporins in kidney. Am. J. Physiol. Renal Physiol. 276: F331–F339, 1999.
- 73. **Meinild, A. K., D. A. Klaerke, and T. Zeuthen.** Bidirectional water fluxes and specificity for small hydrophilic molecules in aquaporins 0–5. *J. Biol. Chem.* 273: 32446–32451, 1998.
- Mitra, A. K., L. J. Miercke, G. J. Turner, R. F. Shand, M. C. Betlach, and R. M. Stroud. Two-dimensional crystallization of *Escherichia coli*-expressed bacteriorhodopsin and its D96N variant: high resolution structural studies in projection. *Biophys. J.* 65: 1295–1306, 1993.
- Mitra, A. K., A. N. van Hoek, M. C. Wiener, A. S. Verkman, and M. Yeager. The CHIP28 water channel visualized in ice by electron crystallography. *Nat. Struct. Biol.* 2: 726–729, 1995.
- 76. Nagelhus, E. A., Y. Horio, A. Inanobe, A. Fujita, F. M. Haug, S. Nielsen, Y. Kurachi, and O. P. Ottersen. Immunogold evidence suggests that coupling if K⁺ siphoning and water transport in rat retinal Muller cells is mediated by a coenrichment of Kir4.1 and AQP4 in specific membrane domains. *Glia* 26: 47–54, 1999.
- Nakhoul, N. L., B. A. Davis, M. F. Romero, and W. F. Boron. Effect of expressing the water channel aquaporin-1 on the CO₂ permeability of *Xenopus* oocytes. *Am. J. Physiol. Cell Physiol.* 274: C543–C548, 1998.
- 78. **Patil, R. V., Z. Han, and M. B. Wax.** Regulation of water channel activity of aquaporin 1 by arginine vasopressin and atrial natriuretic peptide. *Biochem. Biophys. Res. Commun.* 238: 392–396, 1997.
- Prasad, G. V., L. A. Coury, F. Finn, and M. L. Zeidel. Reconstituted aquaporin 1 water channels transport CO₂ across membranes. J. Biol. Chem. 273: 33123–33126, 1998.
- 80. **Preston, G. M., T. P. Carroll, W. B. Guggino, and P. Agre.** Appearance of water channels in *Xenopus* oocytes expressing red cell CHIP28 protein. *Science* 256: 385–387, 1992.
- Preston, G. M., J. S. Jung, W. B. Guggino, and P. Agre. Membrane topology of aquaporin CHIP: analysis of function epitope-scanning mutants by vectorial proteolysis. *J. Biol. Chem.* 269: 1668–1673, 1994.
- Preston, G. M., J. S. Jung, W. B. Guggino, and P. Agre. The mercury-sensitive residue at cysteine 189 in the CHIP28 water channel. *J. Biol. Chem.* 268: 17–20, 1993.
- Preston, G. M., B. L. Smith, M. L. Zeidel, J. J. Moulds, and P. Agre. Mutations in aquaporin-1 in phenotypically normal human without functional CHIP water channels. *Science* 265: 1585–1587, 1994.
- 84. Rash, J. E., T. Yasumura, C. S. Hudson, P. Agre, and S. Nielsen. Direct immunogold labeling of aquaporin-4 in square arrays of astrocyte and ependymocyte plasma membranes in rat brain and spinal cord. *Proc. Natl. Acad. Sci. USA* 95: 11981–11986, 1998.
- Ren, G., P. Melnyk, and A. K. Mitra. Structural analysis of the binding of a mercurial reagent to AQP1 by electron cryocrystallography (Abstract). *Biophys. J.* 76: 137, 1999.
- Schreiber, R., R. Nitschke, R. Greger, and K. Kunzelmann. The cystic fibrosis transmembrane conductance regula-

tor activates aquaporin 3 in airway epithelial cells. *J. Biol. Chem.* 274: 11811–11816, 1999.

- 87. Shahrohk, Z., S. Bicknese, S. B. Shohet, and A. S. Verkman. Single photon radioluminescence. II. Experimental detection and biological applications. *Biophys. J.* 63: 1267–1279, 1992.
- 88. **Shi, L. B., W. R. Skach, T. Ma, and A. S. Verkman.** Distinct biogenesis mechanisms for water channels MIWC and CHIP28 at the endoplasmic reticulum. *Biochemistry* 34: 8250–8256, 1995.
- Shi, L. B., W. Skach, and A. S. Verkman. Functional independence of monomeric CHIP28 water channels revealed by expression of wild type-mutant heterodimers. *J. Biol. Chem.* 269: 10417–10422, 1994.
- Shi, L. B., and A. S. Verkman. Selected cysteine point mutations confer mercurial sensitivity to the mercurialinsensitive water channel MIWC. *Biochemistry* 35: 538–544, 1996
- Skach, W., L. B. Shi, M. C. Calayag, A. Frigeri, V. R. Lingappa, and A. S. Verkman. Topology and biogenesis of the CHIP28 water channel at the endoplasmic reticulum. *J. Cell Biol.* 125: 803–816, 1994.
- Subramaniam, S., M. Gerstein, D. Oesterhelt, and R. Henderson. Electron diffraction analysis of structural changes in the photocycle of bacteriorhodopsin. *EMBO J.* 12: 1–8, 1993.
- 93. **Tamarappoo, B. K., N. Koyama, M. Gabbert, and A. S. Verkman.** High-throughput screening of combinatorial drug libraries to identify non-mercurial aquaporin inhibitors. (Abstract). *J. Am. Soc. Nephrol.* 10:25A, 1999.
- Tamarappoo, B. K., and A. S. Verkman. Defective trafficking of AQP2 water channels in Nephrogenic Diabetes Insipidus and correction by chemical chaperones. *J. Clin. Invest.* 101: 2257– 2267, 1998.
- 95. **Thevenin, B. J. M., N. Periasamy, S. B. Shohet, and A. S. Verkman.** Segmental dynamics of the cytoplasmic domain of erythrocyte band 3 determined by time-resolved fluorescence anisotropy: sensitivity to pH and ligand binding. *Proc. Natl. Acad. Sci. USA* 91: 1741–1745, 1994.
- 96. Tsukaguchi, H., C. Shayakul, U. V. Berger, B. Mackenzie, S. Devidas, W. B. Guggino, A. N. van Hoek, and M. A. Hediger. Molecular characterization of a broad selectivity neural solute channel. J. Biol. Chem. 273: 24737–24743, 1998.
- 97. **Umenishi, F., J. M. Verbavatz, and A. S. Verkman.** cAMP regulated membrane diffusion of a green fluorescent protein-aquaporin-2 chimera measured by photobleaching recovery. *Biophys. J.* In press.
- 98. **Unwin, N.** Acetylcholine receptor channel imaged in the open state. *Nature* 373: 37–43, 1995.
- Unwin, N. The nicotinic acetylcholine receptor of the *Torpedo* electric ray. *J. Struct. Biol.* 121: 181–190, 1998.
- Van Hoek, A. N., and A. S. Verkman. Functional reconstitution of the isolated erythrocyte water channel CHIP28. *J. Biol. Chem.* 267: 18267–18269, 1992.
- 101. Van Hoek, A. N., M. Wiener, S. Bicknese, L. Miercke, J. Biwersi, and A. S. Verkman. Secondary structure analysis of purified CHIP28 water channels by CD and FTIR spectroscopy. *Biochemistry* 32: 11847–11856, 1993.
- 102. Van Hoek, A. N., M. C. Wiener, J. M. Verbavatz, D. Brown, R. R. Townsend, P. H. Lipniunas, and A. S. Verkman. Purification and structure-function analysis of PNGase F- and endo-β-galactosidase-treated CHIP28 water channels. *Biochemistry* 34: 2212–2219, 1995.
- 103. Van Hoek, A. N., B. Yang, S. Kirmiz, and D. Brown. Freeze-fracture analysis of plasma membranes of CHO cells stably expressing aquaporins 1–5. *J. Membr. Biol.* 163: 243–254, 1998.
- 104. Verbavatz, J. M., D. Brown, I. Sabolić, G. Valenti, D. A. Ausiello, A. N. van Hoek, T. Ma, and A. S. Verkman. Tetrameric assembly of CHIP28 water channels in liposomes and cell membranes. A freeze-fracture study. *J. Cell Biol.* 123: 605–618, 1993.
- 105. Verbavatz, J. M., T. Ma, R. Gobin, and A. S. Verkman. Absence of orthogonal arrays in kidney, brain and muscle from

F28

- transgenic knockout mice lacking water channel aquaporin-4. *J. Cell Sci.* 110: 2855–2860, 1997.
- Verkman, A. S. Role of aquaporin water channels in kidney and lung. Am. J. Med. Sci. 316:310–320, 1998.
- Verkman, A. S.. Lessons on renal physiology from transgenic mice lacking aquaporin water channels. *J. Am. Soc. Nephrol.* 10: 1126–1135, 1999.
- Verkman, A. S., and B. Yang. Aquaporin and ion conductance. Science 271: 1491, 1997.
- 109. Walz, T., T. Hirai, K. Murata, J. B. Heymann, K. Mitsuoka, Y. Fujiyoshi, B. L. Smith, P. Agre, and A. Engel. The three-dimensional structure of aquaporin-1. *Nature* 387: 624– 627, 1997.
- 110. Walz, T., B. L. Smith, M. L. Zeidel, A. Engel, and P. Agre. Biologically active two-dimensional crystals of aquaporin CHIP. J. Biol. Chem. 269: 1583–1586, 1994.
- 111. Walz, T., P. Tittmann, K. H. Fuchs, D. J. Muller, B. L. Smith, P. Agre, H. Gross, and A. Engel. Surface topographies at subnanometer-resolution reveal asymmetry and sidedness of aquaporin-1. *J. Mol. Biol.* 264: 907–918, 1996.
- 112. Walz, T., D. Typke, B. L. Smith, P. Agre, and A. Engel. Projection map of aquaporin-1 determined by electron crystallography. Nat. Struct. Biol. 2: 730–732, 1995.
- 113. Wiener, M. C., C. F. Snook, M. E. DiLorenzo, A. S. Verkman, X. Hu, K. Schulten, and A. S. Mitra. Three-dimensional crystallization and preliminary characterization of human aquaporin-1. (Abstract). *Biophys. J.* 76: A277, 1999.
 114. Wistow, G. J., M. M. Pisano, and A. B. Chepelinsky. Tandem
- 114. **Wistow, G. J., M. M. Pisano, and A. B. Chepelinsky.** Tandem sequence repeats in transmembrane channel proteins. *Trends Biochem. Sci.* 16: 170–171, 1991.
- 115. Yang, B., D. Brown, and A. S. Verkman. The mercurial-insensitive water channel (AQP-4) forms orthogonal arrays in stably transfected CHO cells. *J. Biol. Chem.* 271: 4577–4580, 1996.
- 116. Yang, B., N. Fukuda, A. N. van Hoek, M. A. Matthay, T. Ma, and A. S. Verkman. Permeability of aquaporin-1 to carbon dioxide measured in erythrocytes and lung of wildtype vs. aquaporin-1 null mice and in reconstituted proteoliposomes. *J. Biol. Chem.* In press.

- 117. **Yang, B., A. N. van Hoek, and A. S. Verkman.** Very high single channel water permeability of aquaporin-4 in baculovirus-infected Sf9 cells and liposomes reconstituted with purified aquaporin-4. *Biochemistry* 36: 7625–7632, 1997.
- 118. Yang, B., and A. S. Verkman. Water and glycerol permeability of aquaporins 1–5 and MIP determined quantitatively by expression of epitope-tagged constructs in *Xenopus* oocytes. *J. Biol. Chem.* 272: 16140–16146, 1997.
- 119. **Yang, B., and A. S. Verkman.** Urea transporter UT3 functions as an efficient water channel: direct evidence for a common water/urea pathway. *J. Biol. Chem.* 273: 9369–9372, 1998.
- 120. Yasui, M., T. H. Kwon, M. A. Knepper, S. Nielsen, and P. Agre. Aquaporin 6: an intracellular vesicle water channel protein in renal epithelia. *Proc. Natl. Acad. Sci. USA* 96: 5808–5813, 1999.
- 121. **Yool, A. J., W. D. Stamer, and R. W. Regan.** Forskolin stimulation of water and cation permeability in aquaporin 1 water channels. *Science* 273: 1216–1218, 1996.
- 122. Zeidel, M. L., S. V. Ambudkar, B. L. Smith, and P. Agre. Reconstitution of functional water channels in liposomes containing purified red cell CHIP28 protein. *Biochemistry* 31: 7436–7440, 1992.
- 123. Zhang, P., C. Toyoshima, K. Yonekura, N. M. Green, and D. L. Stokes. Structure of the calcium pump from sarcoplasmic reticulum at 8-Å resolution. *Nature* 392: 835–839, 1998.
- 124. **Zhang, R., S. Alper, B. Thorens, and A. S. Verkman.** Evidence from oocyte expression that the erythrocyte water channel is distinct from band 3 and the glucose transporter. *J. Clin. Invest.* 88: 1553–1558, 1991.
- 125. Zhang, R., K. Logee, and A. S. Verkman. Expression of mRNA coding for kidney and red cell water channels in *Xenopus* oocytes. *J. Biol. Chem.* 265: 15375–15378, 1990.
- 126. Zhang, R., W. Skach, H. Hasegawa, A. N. van Hoek, and A. S. Verkman. Cloning, functional analysis and cell localization of a kidney proximal tubule water transporter homologous to CHIP28. J. Cell Biol. 120: 359–369, 1993.
- 127. Zhang, R., A. N. van Hoek, J. Biwersi, and A. S. Verkman. A point mutation at cysteine 189 blocks the water permeability of rat kidney water channel CHIP28k. *Biochemistry* 32: 2938– 2941, 1993.